

# Dual Harnessing of Air Conditioning Exhaust: PV Cooling and Dishwasher Drying

Charbel Habchi<sup>a</sup>, Fadl Moukalled<sup>b</sup>, Mahmoud Khaled<sup>c,d,\*</sup>

<sup>a</sup> Multiphysics Interaction Lab (MiLab), Los Angeles, CA 90703, USA

<sup>b</sup> American University of Beirut, Mechanical Engineering Department, P.O. Box 11-0236 Riad El Solh, Beirut, Lebanon

<sup>c</sup> Energy and Thermo-Fluid Group, Lebanese International University LIU, Bekaa, Lebanon

<sup>d</sup> Center for Sustainable Energy and Economic Development (SEED), Gulf University for Science and Technology, Kuwait

## ARTICLE INFO

### Keywords:

Hybrid PV/T  
PV cooling  
Waste heat recovery  
Energy and exergy analysis  
Fabric drier

## ABSTRACT

This paper investigates the potential of utilizing air-conditioning (AC) system exhaust to cool Photo Voltaic (PV) panels, leading to improved efficiency. Additionally, the study explores harnessing the heat emitted from the PV modules for thermal applications. Numerical simulations demonstrate that this cooling method can enhance PV module efficiency by 5% to 50% compared to non-cooled scenarios. Moreover, the recovered hot air leaving the PV panels is directed to a dishwasher for drying purpose, thereby optimizing the overall energy utilization of the proposed system. An energetic and exergetic analysis of the recuperated thermal energy showcases its exceptional thermal efficiency, ranging from 98% to 45%, which aligns with values reported in existing literature. The exergetic efficiency of the suggested system falls between 5.2% and 1%, consistent with the range of values documented in previous studies. By exploiting AC system exhaust and waste heat, this new approach can significantly enhance the performance of PV panels and promote energy efficiency. Implementing this technology could prove instrumental in sustainable energy applications.

## 1. Introduction

The rapid growth of industrial and economic activities has led to an increasing demand for energy, primarily from fossil fuels. This surge in fuel consumption has had detrimental effects on the ecological system [1–8]. In this context, sustainable development practices have become crucial, with an emphasis on utilizing renewable and non-polluting energy sources, such as solar energy [9–15].

Solar energy systems can be categorized into two main types:

1. Thermal energy production through solar collectors [16,17].
2. Electricity generation using photovoltaic panels (PV) [18,19].

This study focuses on a combination of both technologies, denoted as photovoltaic/thermal (PV/T) systems [20,21].

PV panels, being semiconductors, they require sunlight to generate electricity, but their efficiency decreases with rising surface temperatures [22,23]. Studies have shown that for every 1°C increase in surface temperature, PV panel efficiency drops by about 0.5% [24]. To address this issue, this paper proposes a new method to enhance the efficiency of PV panels by reducing their surface temperature through enhanced cooling using the exhaust air of Air Conditioning (AC) systems. This cooling method involves directing the air flow over the back side of

the PV panel. The proposed system is suitable for both industrial and residential applications, particularly benefiting communities in hot climate regions. Furthermore, the heated air exiting the PV panels can be utilized for thermal applications [25,26].

The cooling of photovoltaic panels has garnered significant attention, becoming a prominent research area within the PV system domain. It mainly focuses on two key aspects [27,28]:

1. Enhancing the efficiency of PV panels by reducing their surface temperature.
2. Recovering the energy of the working fluid exiting the PV panels.

Numerous cooling systems for PV panels have been reported [29,30], involving different working fluids and flow configurations, as discussed in the following.

Elminshawy *et al.* [31] highlighted the importance of a cooling strategy for floating photovoltaic systems using surrounding water to prevent performance deterioration and increase system lifespan. The experimental study examined a novel passive cooling approaches, highlighting a partially submerged floating system with attached fins as superior to traditional systems, achieving a 19% reduction in operating temperature and a 24% increase in output power at a submerged area ratio of 20%. In another study, Elminshawy *et al.* [32] investigated the management of

\* Corresponding author.

E-mail address: [mahmoud.khaled@liu.edu.lb](mailto:mahmoud.khaled@liu.edu.lb) (M. Khaled).

<https://doi.org/10.1016/j.enbenv.2023.11.003>

Received 17 August 2023; Received in revised form 10 November 2023; Accepted 11 November 2023

Available online xxx

2666-1233/Copyright © 2023 Southwest Jiatong University. Publishing services by Elsevier B.V. on behalf of KeAi Communication Co. Ltd. This is an open access article under the CC BY-NC-ND license (<http://creativecommons.org/licenses/by-nc-nd/4.0/>)

the operating temperature of solar photovoltaic concentrator systems to maintain their efficiency. Their study explores the use of two coolants, pure water and water-based aluminum oxide nanofluids, and suggests that a ducting channel arrangement can effectively cool the C-PV module, with the 0.7% Al<sub>2</sub>O<sub>3</sub>-nanofluid significantly improving electrical and thermal efficiencies by 10% and 36%, respectively.

Moharram *et al.* [33] developed a water cooling system for PV panels in hot dry regions, aiming to minimize water and electricity consumption. However, their system has drawbacks, including the use of an electric water pump, water evaporation in hot environments (such as deserts), and the inability to integrate PV panels with a thermal system for additional benefits.

An alternative approach proposed by Assi *et al.* [34] involves a passive forced air cooling system using air exhausted from an air conditioning (AC) system, flowing over the front surface of the PV panel. This system has the advantage of combining dust removal with panel cooling, and it doesn't require external power as the flow is driven by the AC unit fans. However, recuperating the hot air at the trailing edge of the PV panel is challenging with this design. Othman *et al.* [24] presented novel PV/T technologies, where PV panels are cooled by forced air or water flow, and the recuperated fluid is employed for thermal applications. They also introduced PV/T collectors with V-grooves to overcome the reduction in electric efficiency caused by the presence of a glass cover. Other research efforts have explored cooling PV panels using converging channel flow configurations in hot and dry climate regions, vapor directed normally to the backside of the PV panel [35], and combining wind and solar energy in a single system [36], among other techniques [37].

This study introduces a novel approach by harnessing the exhaust air from air conditioning (AC) systems to act as a natural coolant, gently flowing over the rear surface of photovoltaic (PV) panels. This innovative method eliminates the need for supplementary fans or added power consumption. Additionally, this new design enables the recapture of heated air that would otherwise escape from the PV panel, repurposing it for drying applications. This dual functionality not only contributes to a noteworthy reduction in both the carbon footprint, but also yields cost savings on electricity bills.

The paper is organized as follows: in section 2, the proposed solution for the PV cooling and waste heat recovery is discussed along with the numerical method adopted. The results are discussed in section 3 followed by the concluding remarks in section 4.

## 2. Materials and Methods

### 2.1. Proposed Solution

Various types of PV panels are available in the market, each comprising multiple layers and exhibiting different performance characteristics based on the physical properties of these layers and the manufacturing technology used [38]. For the present study, the polycrystalline BP Solar BP350 panel [39] is used which consists of six layers.

The topmost layer features a tempered ultra-clear glass cover, as depicted in Fig. 1. This specialized glass possesses high transmittance and low iron content. Immediately below the glass, there is an anti-reflective

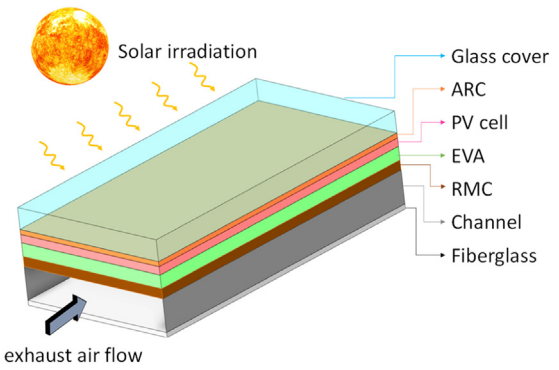


Fig. 1. Schematic view of the different layers of the modified PV panel.

coating (ARC) that facilitates the easy transmission of incoming photons to the PV cells located just beneath it. These PV cells are made of polycrystalline material and are coated with silicon nitride (SiN).

To secure the PV cells and provide electrical isolation, ethylene vinyl acetate (EVA) is utilized. The rear metal contact (RMC) is employed as an additional protective layer for the PV cells. Traditionally, a Tedlar polymer layer is placed on the backside of the RMC, providing additional insulation and moisture protection. However, in the present study, this layer has been omitted to enable effective cooling of the system. Consequently, the exhausted air from the AC system is directed below the RMC and confined between the RMC and a layer of fiberglass. The fiberglass minimizes heat exchange with the ambient air, ensuring that the coolant only exchanges heat with the upper wall, which effectively cools down the PV cells.

In Table 1, the dimensions (thickness) and thermophysical properties of the different layers of the PV panel are provided, as adapted from Armstrong *et al.* [40]. The two additional layers introduced in the current study are for the air flow channel and the fiberglass layer.

The width and length of the flow channel for one PV panel are 537 mm and 839 mm, respectively, corresponding to the surface area of the PV module. Since the width is much greater than the height of the channel (ratio around 119), a two-dimensional assumption is made for the fluid flow simulations.

The proposed cooling system is visually represented in Fig. 2. To operate this system, the air conditioning (AC) equipment employs a mass flow rate denoted by  $\dot{m}$  to cool and dehumidify the air. This conditioned air is then supplied to the space at a temperature of approximately 13°C during the summer season. The supply air temperature is a design parameter that can be adjusted by varying the air mass flow rate. Therefore, there exists a trade-off between the air supply temperature and the air mass flow rate, allowing for flexibility in achieving the desired cooling effect.

Within the conditioned space, the supply air serves to maintain a comfortable temperature of about 23°C, adhering to ASHRAE guidelines for human thermal comfort [41]. A portion of the air, represented by the fraction  $(1 - x)$ , is recirculated back to the supply unit for reuse in the cooling process. Meanwhile, the remaining fraction  $(x)$  can either be

Table 1  
PV panel layers and their thermophysical properties.

Layer	Thickness (mm)	Thermal conductivity $k$ (W/m.K)	Density $\rho$ (kg/m <sup>3</sup> )	Specific thermal capacity $c_p$ (J/kg.K)
Glass cover	3	1.8	3000	500
ARC	10 <sup>-4</sup>	32	2400	691
PV cell	0.23	148	2330	677
EVA	0.5	0.35	960	2090
Rear contact	0.01	237	2700	900
Airflow channel	45	0.024	1.23	1005
Fiberglass	5	0.034	45	843

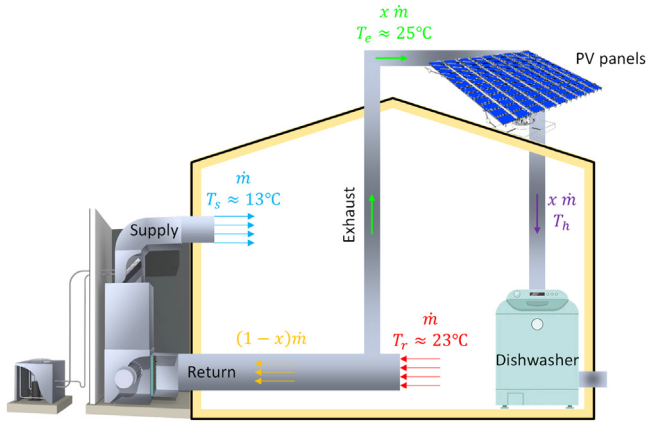


Fig. 2. Schematic view of the cooling system using the exhaust AC air for PV cooling and providing hot air to the dishwasher.

discarded or directed towards a thermal wheel for waste heat recovery. The specific value of the exhausted fraction ( $x$ ), which is replaced by fresh air for ventilation purposes, depends on the type of occupancy in the space. For instance, in hospitals,  $x = 1$ , meaning all the air is replaced, while in residences,  $x = 0.1$ , signifying only a small portion is replaced to ensure proper ventilation.

Therefore, the exhausted air from the air conditioning (AC) system is utilized to cool the PV panels. This is achieved by directing the air leaving the exhaust grill into a nozzle, which is then connected to the PV panel. The exhaust air entering the nozzle is assumed to have a temperature of  $25^\circ\text{C}$ , resulting from heat gain from the ambient air. Once the air exits the nozzle, it flows over the back of the PV panel within a specially designed channel (Fig. 1). To enhance the heat exchange between the air flow and the PV panel, the lower side of the coolant channel is constructed with fiberglass insulation.

Notably, this innovative system operates without the need for any additional power, as the cold air is propelled by the extraction fan of the AC system. Furthermore, the air leaving the PV panel becomes hot, presenting an opportunity for its utilization in thermal applications.

It is important to note that in this setup, the connections from the exhaust grill to the air channel inlet and from the channel exit to the heat recovery system are well insulated.

This cooling system proves highly efficient, particularly in hot regions where AC usage is frequent. Consequently, the feasibility and effectiveness of this concept in two cities, namely Beirut and Doha, is examined. The subsequent section will delve into the numerical method, boundary conditions, and considerations of weather conditions and air flow rates.

## 2.2. Numerical Procedure

The flow field within the cooling channel is governed by the steady-state Reynolds-averaged Navier-Stokes (RANS) equations, along with the energy equation for incompressible flow. To capture the effects of turbulence, the  $SST \kappa - \omega$  turbulence model [42] is employed, computing the Reynolds stress tensor resulting from the averaging process on the nonlinear convective terms in the momentum equation.

Sequentially solving the flow and energy equations, a second-order accurate central-difference scheme is used for the diffusion terms, while a second-order upwind scheme handles the convective terms. To resolve the coupling between pressure and velocity, the Coupled algorithm is employed.

For meshing, a nonuniform quadrilateral structured mesh is utilized, with special emphasis on grid refinement at the wall boundaries to accurately capture the high velocity and temperature gradients in these

regions. In particular, the highest dimensionless wall distance ( $y^+$ ) does not exceed 1, ensuring appropriate modeling of the viscous sub-layer.

To achieve grid-independent solutions, the solver is executed with increasing mesh densities until the results show no significant effects. Validation is conducted following the approach proposed by Celik *et al.* [43]. Considering that heat transfer is significantly affected by near-wall behavior, grid independence is verified by calculating the convective heat transfer coefficient ( $h$ ) and the wall shear stress ( $\tau_w$ ). The analysis indicates an uncertainty of approximately 0.3% in the fine-grid solution. It should be noted that the mesh study was carried out for a single PV panel at the highest Reynolds number, where the highest discretization error is anticipated.

## 2.3. Boundary Conditions

The new concept of cooling the PV panels is put to the test on a residential house with a floor area of  $200 \text{ m}^2$ . The sensible cooling load for the space is estimated at  $\dot{q} = 43.75 \text{ kW}$ , with an air supply temperature of  $T_s = 13^\circ\text{C}$  and an indoor air temperature maintained at  $T_D = 13^\circ\text{C}$  [44]. Accordingly, the required air mass flow rate for cooling the house, calculated using  $\dot{m} = \dot{q}/[c_p(T_d - T_s)]$  is found to be around  $4.35 \text{ kg/s}$ . Considering residential occupancy, the extracted air fraction is 0.1, and thus the mass flow rate utilized for cooling the PV panels is  $0.435 \text{ kg/s}$ .

The study considers two cities, Beirut and Doha, with their annual average weather data adopted from References [45,46], respectively. Beirut experiences a Mediterranean climate with dry hot summers and mild winters, while Doha has a hot desert climate.

At the inlet to the cooling channel, uniform velocity and temperature profiles are applied, and atmospheric pressure is set at the outlet. The conduction equation is solved in all PV layers, and the internal surfaces of the channel are linked to convective heat transfer and airflow. The bottom surface of the PV panel, in contact with the external wind, is assumed shaded, while the upper surface is subjected to wind and solar radiation.

To model the convective heat transfer coefficient between the back surface and the ambient air, the following equation, based on Sharples and Charlesworth [47], is employed:

$$h_{o, \text{back}} = 2.2V_{\text{wind}} + 8.3 \quad (1)$$

While neglecting solar radiation, heat transfer from the back surface is treated as a convective boundary condition with the air temperature and speed obtained from weather data.

On the front surface, heat transfer is affected by both solar radiation and convection with the ambient air. To accurately assess the energy balance, solar radiation absorbed by the exterior surface of a wall or roof is considered, and an alternative method, utilizing the sol-air temperature ( $T_e$ ), is applied. The sol-air temperature is defined as the fictitious outdoor dry-bulb temperature, such that in the absence of solar radiation, the surface exchanges the same net amount of energy with the air at the sol-air temperature as it does in the actual environment [48].

The heat flux into the surface, considering sunlit conditions, is given by [48]:

$$q = \alpha I_t + h_{o, \text{front}}(T_o - T_s) - \epsilon \Delta R \quad (2)$$

where  $\alpha$  is the solar absorptivity coefficient,  $I_t$  is the total solar radiation incident on the surface ( $\text{W/m}^2$ ),  $h_{o, \text{front}}$  is the exterior film coefficient ( $\text{W/m}^2 \cdot \text{K}$ ), and  $\epsilon \Delta R$  is the radiation correction factor ( $\text{W/m}^2$ ).

The sol-air temperature ( $T_e$ ) is then determined using the following expression [48]:

$$T_e = T_o + \frac{\alpha I_t}{h_{o, \text{front}}} - \frac{\epsilon \Delta R}{h_{o, \text{front}}} \quad (3)$$

The exterior film coefficient is calculated as the sum of the convective heat transfer coefficient ( $h_{\text{convection}}$ ) and the radiative heat transfer coefficient ( $h_{\text{radiation}}$ ). The radiative heat transfer coefficient is assumed

**Table 2**  
Calculated ambient and boundary conditions.

City	$T_{in}$ °C	$T_o$ °C	$T_e$ °C	$I_t$ (W/m <sup>2</sup> )	$V$ (m/s)	$h_{o,front}$ (W/m <sup>2</sup> K)	$h_{o,back}$ (W/m <sup>2</sup> K)
Beirut	25	32.8	79.8	988	4.2	25.4	17.5
Doha	25	40.1	86.3	973	4.6	26.9	18.5

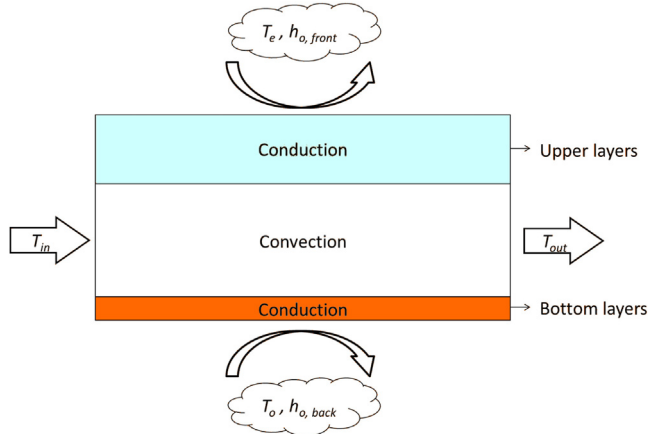


**Fig. 3.** Illustration of the boundary conditions for the cooled PV panel.

constant at 5.11 W/m<sup>2</sup>.K according to Rowley and Eckley [49]. The convective heat transfer coefficient is determined based on the wind speed using the correlation proposed by Sharples [47]:

$$h_{convection} = 3.3V_{wind} + 6.5 \quad (4)$$

The boundary conditions used in the study are summarized in Fig. 3.

Simulations are conducted for August 1st at 12:00 pm in the two cities, Beirut and Doha, as considered in this study. Table 2 presents the temperatures, solar radiation, and heat transfer coefficients for both cities, obtained from the previously mentioned models.

Once the temperature of the PV cells ( $T_c$ ) is computed through the CFD simulation, the cell electric efficiency ( $\eta_{el}$ ) is calculated using the relation developed by Evans [50]:

$$\eta_{el} = \eta_{ref} [1 - \beta_{ref}(T_c - T_{ref})] \quad (5)$$

In this equation,  $\eta_{ref} = 11\%$  represents the reference efficiency at standard laboratory conditions,  $T_{ref} = 25^\circ\text{C}$  is the reference temperature, and  $\beta = 0.005 \text{ K}^{-1}$  is the reference temperature coefficient [39]. This computation enables us to evaluate the electric efficiency of the PV cells under the specific thermal conditions encountered in Beirut and Doha during the given time and date.

### 3. Results

#### 3.1. Validation

The numerical predictions are initially compared with theoretical calculations performed for a PV panel without cooling. In the theoretical approach, a one-dimensional thermal resistance network is utilized to model the PV layers. The same boundary conditions mentioned earlier are applied here, but without the presence of a channel and fiberglass insulation layer, focusing solely on the PV layers.

The comparison of cell temperature and efficiency between the CFD and theoretical results is presented in Table 3. The table clearly demonstrates that the differences in cell temperature and efficiency obtained from the two methods do not exceed 0.4% and 0.2%, respectively. Additionally, it is noteworthy that the cell temperature experiences significant increase in both cities, leading to a reduction in cell efficiency from 11.1% under standard conditions to 9.13% and 8.75% for the weather conditions in Beirut and Doha, respectively.

**Table 3**  
Comparison of temperature and cell efficiency obtained from CFD simulations for a PV module without cooling with theoretical calculations using a one-dimensional thermal resistance network.

City	Theoretical		CFD		% Difference	
	$T_c$ °C	$\eta_{el}$ (%)	$T_c$ °C	$\eta_{el}$ (%)	$T_c$ °C	$\eta_{el}$ (%)
Beirut	60.3	9.1	60.5	9.1	0.4	0.2
Doha	67.1	8.8	67.4	8.8	0.4	0.2

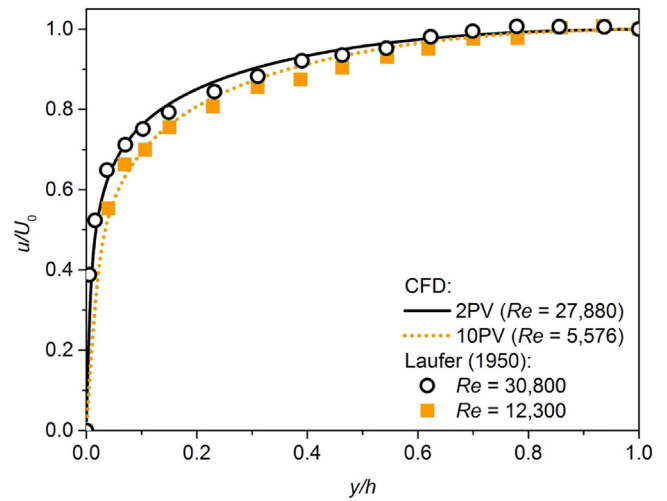


**Fig. 4.** Comparison of mean velocity profiles at the PV outlet obtained from the current CFD simulations with experimental data from Laufer [51].

The CFD results are further validated by comparing the mean velocity profile at the outlet section with a similar one obtained experimentally by Laufer [51] for flow in a two-dimensional channel. For this comparison, the cases of 2 and 10 PV panels are considered, as the flow does not reach a fully developed state at the outlet for 1 PV panel. Fig. 4 illustrates the agreement between the numerical and experimental profiles, with the maximum relative error between predictions and measurements not exceeding 4%.

#### 3.2. PV cooling

In this section, the impact of cooling on the performance of the PV panels is assessed, focusing on hot summer days as cooling becomes significant during such periods, while it remains less influential in winter due to relatively low ambient air temperatures.

The streamwise variations in the surface temperature of the PV panels for the two cities under study, Beirut and Doha, are presented in Fig. 5. When cooling is not applied, i.e., cooling is solely provided by wind as described in section 2, the temperature of the PV panels reaches its highest values, approximately 60°C in Beirut and 67°C in Doha. Upon implementing the cooling system, it is evident that the temperature of the PV panels in both cities remains below the maximum temperature obtained without cooling, particularly for a small number of PV panels.

Locally, it is observed that the temperature initially rises sharply from the leading edge of the PV panels until a distance of  $x/L = 0.1$ . Be-

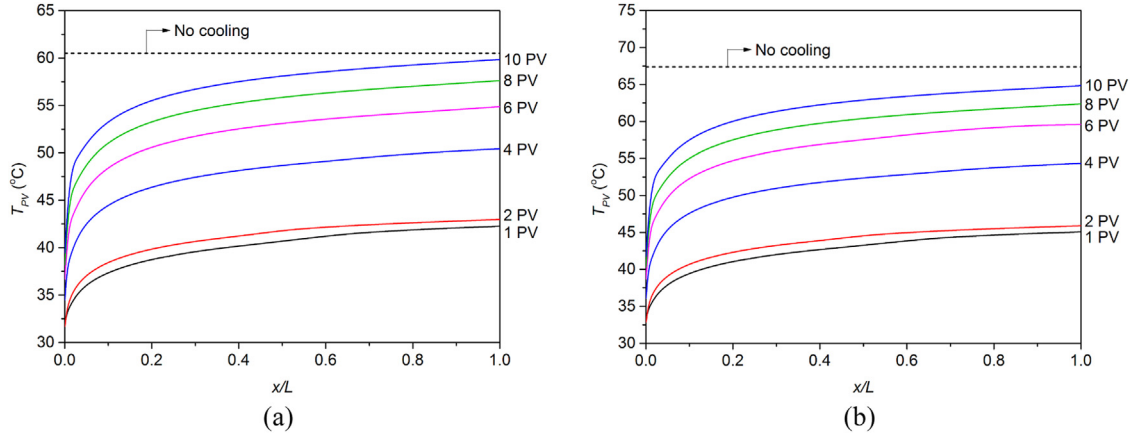


Fig. 5. Streamwise variation of the surface temperature of PV panels for (a) Beirut and (b) Doha cities.

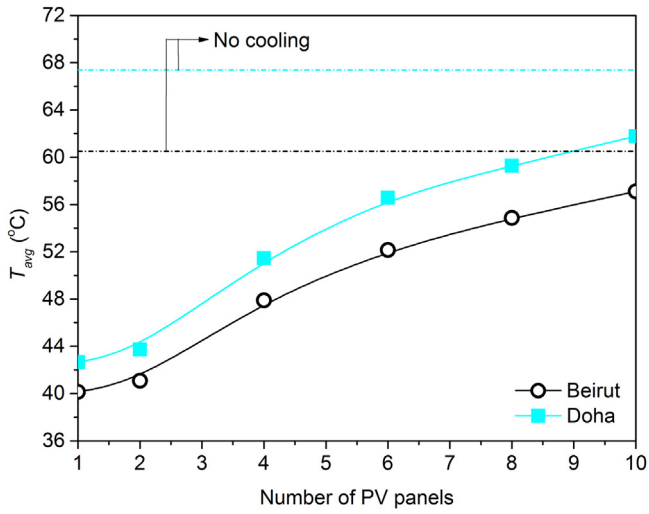


Fig. 6. Average surface temperature of PV panels for various numbers of panels.

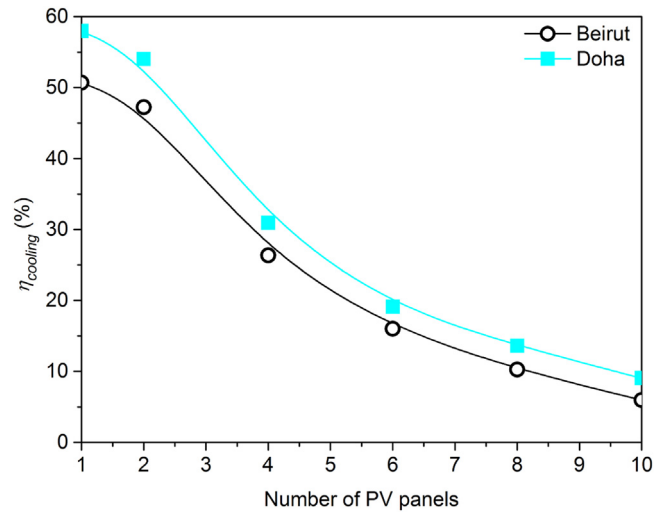


Fig. 7. Relative enhancement of the cooling system obtained from Eq. (6).

yond that point, the rate of temperature increase is significantly lower. On average, nearly 90% of the maximum temperature is reached over 10% of the PV panel length, while the remaining 10% increase occurs over the remaining 90% of the panel length. Moreover, as the number of PV panels increases, the temperature also rises, indicating that cooling becomes less efficient.

The effect of the number of PV panels on the cooling process is illustrated in Fig. 6. Here,  $T_{avg}$  represents the area-weighted average of the PV surface temperature. It can be observed that the average surface temperature of the panels in Doha city is higher than that in Beirut city, owing to harsher weather conditions. The average temperature increases by approximately 1.4 times when the number of PV panels increases from 1 to 10.

Despite these increases, in all cases, the predicted surface temperature of the PV panels is lower than the value obtained without cooling. As shown in Fig. 7, the relative enhancement of the cooling process, calculated according to Equation (6), ranges from 49% to 56% for one PV panel and decreases to approximately 4% to 7% when the number of panels reaches 10. This efficiency of the cooling process reduces with increasing the number of PV panels, as the heat exchange area becomes larger.

$$\eta_{cooling} = \frac{T_{no\ cooling} - T_{cooling}}{T_{no\ cooling}} \quad (6)$$

### 3.3. PV electric efficiency

To underscore the significance of the new cooling system on the electric efficiency of the PV modules, the cell efficiency is calculated using Equation (5) and plotted in Fig. 8 for different numbers of PV panels. The dotted lines in the same figure represent the cell efficiency in case of no cooling, with values around 8.75% for Doha city and 9.1% for Beirut.

Fig. 8 shows that the cooling process substantially enhances the cell efficiency, reaching approximately 10.1% to 10.25% for 1 PV module. As the number of PV panels increases, this efficiency decreases but remains higher than the value obtained without cooling. The relative increase in cell electric efficiency ranges from 15% for 1 PV module to around 3% for 10 PV modules.

### 3.4. PV/T thermal efficiency

This section focuses on the recovery of the hot air discharged from the cooling channel integrated into the back side of the PV module, which can be utilized for residential applications. To assess the thermal performance of the new system, it is important to calculate the overall thermal efficiency using the following expression:

$$\eta_{th} = \frac{\dot{m}c_p(T_{out} - T_{in})}{I_t N A_{PV}} \quad (7)$$

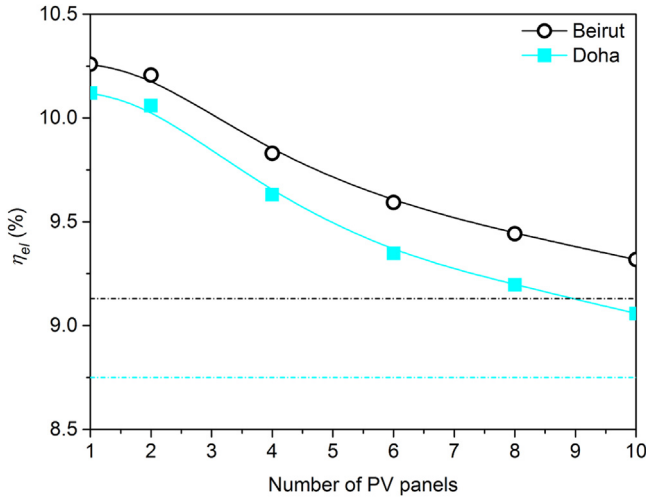


Fig. 8. PV panels electric efficiency.

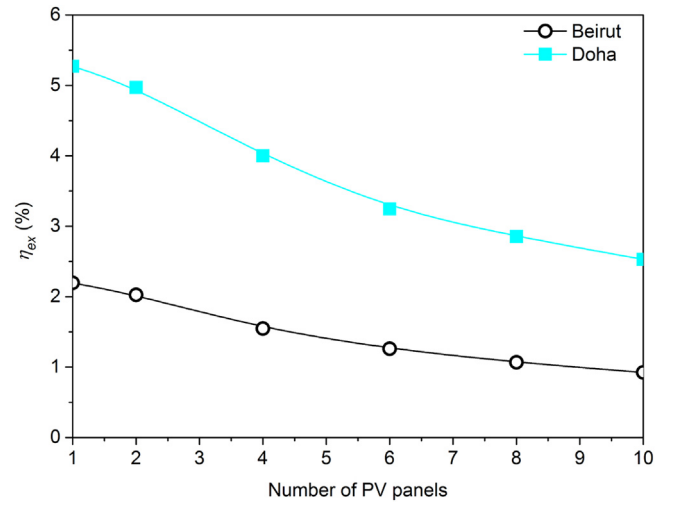


Fig. 10. PV panels exergetic efficiency.

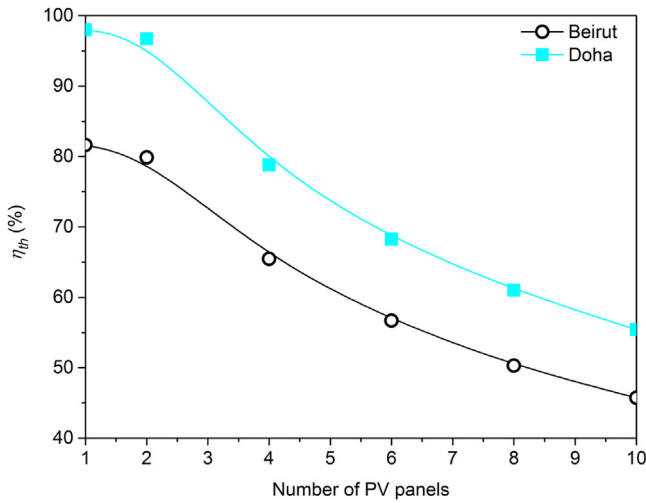


Fig. 9. PV panels thermal efficiency.

where  $T_{out}$  and  $T_{in}$  represent the bulk temperatures at the outlet and inlet of the cooling channel, respectively.  $A_{PV}$  and  $N$  are the surface area and number of PV modules, respectively.

As depicted in Fig. 9, the thermal efficiency can reach high values, up to 98%, for 1 PV module in the hotter region (Doha). However, this efficiency decreases to around 45% in Beirut and 55% in Doha when the number of PV panels increases. It is worth noting that the thermal efficiency of various systems reported in the open literature ranges between 70 and 85% [24,37,52]. The relatively high thermal efficiency value observed here is attributed to the very high ambient air temperature in these hot climate regions, which significantly reduces heat losses from the cooling channel, thus enhancing thermal efficiency.

### 3.5. PV/T exergetic efficiency

Exergy, representing the maximum attainable thermal energy relative to the ambient air temperature, is a widely used metric for analyzing and optimizing PV/T (photovoltaic/thermal) systems [53,54].

According to Bejan [55], the exergetic efficiency can be expressed as follows:

$$\eta_{ex} = \frac{\dot{m}c_p \left[ T_{out} - T_{in} - T_o \ln \left( \frac{T_{out}}{T_{in}} \right) \right] - \dot{m} \frac{\Delta p}{\rho}}{I_t N A_{PV} \left( 1 - \frac{T_o}{T_{app}} \right)} \quad (8)$$

Here,  $T_{out}$  and  $T_{in}$  represent the bulk temperatures at the outlet and inlet of the cooling channel, respectively.  $T_o$  is the ambient air temperature,  $\Delta p$  is the pressure drop across the cooling channels, and  $T_{app}$  is the apparent sun temperature, corresponding to 75% of the black-body temperature of the sun ( $T_{app} = 4333.5$  K) [55].  $A_{PV}$  and  $N$  are the surface area and number of PV modules, respectively.

Fig. 10 illustrates that the exergetic efficiency can reach a maximum value of about 5.2% for 1 PV module in Doha and 2.2% in Beirut. In general, the exergetic efficiency tends to be higher when the ambient air temperature is lower. As the number of PV panels increases, this efficiency decreases to around 2.4% and 1% for Doha and Beirut cities, respectively. It is worth noting that the exergetic efficiency of various systems reported in the literature typically ranges between 5 and 20% [53,54].

### 3.6. Dishwasher drying

In this section, the drying for the dishwasher provided by the hot air leaving the PV/T system is described. In common dishwashers, the water used could be around 20 kg. At the end of the washing cycle, about 0.4% of the water remains on the surface of the dishes ( $m_{wf} = 0.8$  kg) [56]. Therefore, a drying cycle is usually used at the end of the washing process to dry the remaining water from the dishes. This drying cycle is very power consuming. For instance, assuming the enthalpy of evaporation of water around  $h_{fg} = 2400$  kJ/kg [57], the power needed to dry the dishes in a one-hour heating cycle would be around  $q_{dry} = 0.5$  kW. For a household using the dishwasher 5 times in a week for 90 minutes each time, this leads to a total of 150 kWh monthly electric power consumption. The corresponding  $CO_2$  index could range from 60 to 135 kg  $CO_2$ . Moreover, assuming an average price of 10 cents per kWh, this leads to about 15 USD every month.

Thus, the present system uses green energy from the hot air leaving the PV/T system. This hot air is directed to the dishwasher and blown over the wet dishes. Thus, assuming a convection coefficient of  $h = 100$  W/m<sup>2</sup>K and total dishes surface area of 1 m<sup>2</sup>, the time required to dry the dishes is calculated using the hot air from the PV/T as follows:

$$t = \frac{m_{wf} h_{fg}}{h A_{dishes} (T_{air} - T_{dishes})} \quad (8)$$

where  $T_{air}$  is the air temperature leaving the PV/T and  $T_{dishes}$  25°C is the dishes temperature at the end of the washing process.

Fig. 11 shows the time to dry obtained using different numbers of PV panels. As it can be seen from this figure, the time decreases with increasing numbers of PV from around 7 hours to around 1 hour. In fact,

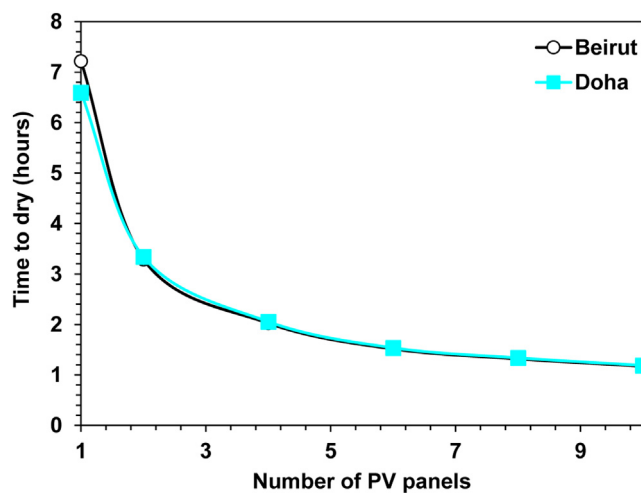


Fig. 11. Time to dry for different numbers of PV panels.

when the number of PV increases, the air temperature leaving the PV/T system is higher, thus leading to better drying process. This highlights the efficiency of the proposed system to recover the waste heat in a direct residential application pertaining to dishwasher drying.

#### 4. Conclusion

This paper presents a new method for enhancing the efficiency of photovoltaic (PV) panels by reducing their surface temperature through enhanced cooling using the exhaust air of air conditioning (AC) systems. The proposed system utilizes the exhausted air from the AC system as a coolant, flowing over the backside of the PV panel. The cooling system operates without the need for any additional power, as the cold air is propelled by the extraction fan of the AC system. Furthermore, the heated air leaving the PV panel is utilized for thermal applications, in the present case as assistance in dishwasher drying.

The numerical simulations conducted to evaluate the proposed cooling system show promising results. The cooling process substantially reduces the surface temperature of the PV panels, leading to an increase in their electric efficiency. The relative enhancement of the cooling system ranges from 49% to 56% for one PV panel, decreasing to approximately 4% to 7% when the number of panels reaches 10. The electric efficiency of the PV panels is also enhanced, with an increase ranging from 15% for 1 PV module to around 3% for 10 PV modules.

Additionally, the proposed cooling system enables the recovery of hot air discharged from the cooling channel, which can be utilized for residential applications. The thermal efficiency of the system can reach up to 98% for 1 PV module in hot climate regions. The exergetic efficiency, which represents the maximum attainable thermal energy relative to the ambient air temperature, ranges from 2.2% to 5.2% for different numbers of PV panels.

Furthermore, the proposed system offers a green energy solution for dishwasher drying, using the hot air leaving the PV/T system to dry the dishes. The time required to dry the dishes decreases with increasing numbers of PV panels, from around 7 hours to around 1 hour. For instance, considering a household running the dishwasher 90 minutes five times a week, this results in a monthly electricity consumption of 150 kWh. The associated  $CO_2$  emissions can reach around 135 kg, with an approximately \$15 per month in electric power bill expenses.

Overall, this study demonstrates the feasibility and effectiveness of the proposed cooling system in enhancing the efficiency of PV panels and recovering waste heat for practical residential applications. The integration of PV/T systems with residential appliances, such as dishwashers, presents an environmentally friendly approach to utilize renewable energy and reduce greenhouse gas emissions. Further research and de-

velopment in this area could lead to significant advancements in sustainable energy practices and contribute to global efforts in mitigating climate change and promoting sustainable development. For instance, future work in this area should encompass real-world testing to validate system performance, cost reduction efforts for increased accessibility, user-friendly integration methods for wider adoption, efficient monitoring and maintenance systems, and collaborative efforts with policymakers to establish incentives and regulations. This complete approach is essential to ensure the effective deployment and long-term success of the proposed cooling system, which not only enhances PV panel efficiency but also contributes to waste heat recovery and reductions in greenhouse gas emissions.

#### Funding Statement

The authors received no specific funding for this study.

Availability of Data and Materials: The data that support the findings of this study are available from the corresponding author, M.K., upon reasonable request.

#### Declaration of Competing Interest

The authors declare that they have no known competing financial interests or personal relationships that could have appeared to influence the work reported in this paper.

#### CRedit authorship contribution statement

**Charbel Habchi:** Conceptualization, Data curation, Formal analysis, Investigation, Methodology, Validation, Writing – original draft, Project administration, Supervision. **Fadi Moukalled:** Conceptualization, Methodology, Formal analysis, Investigation, Writing – review & editing. **Mahmoud Khaled:** Conceptualization, Methodology, Formal analysis, Investigation, Writing – review & editing.

#### References

- [1] S. Ghanimeh, C. Abou Khalil, C. Bou Mosleh, C. Habchi, Optimized anaerobic-fermentative system for the treatment of food waste and wastewater, *Waste Manag.* 71 (2018) 767–774, doi:10.1016/j.wasman.2017.06.027.
- [2] M. Khaled, F. Harambat, H. El Hage, H. Peerhossaini, Spatial optimization of an underhood cooling module – Towards an innovative control approach, *Appl. Energy*. 88 (2011) 3841–3849, doi:10.1016/J.APENERGY.2011.04.025.
- [3] C. Habchi, A. Ghanem, T. Lemenand, D. Della Valle, H. Peerhossaini, Mixing performance in Split-And-Recombine Milli-Static Mixers—A numerical analysis, *Chem. Eng. Res. Des.* 142 (2019) 298–306, doi:10.1016/j.cherd.2018.12.010.
- [4] H. Jaber, M. Ramadan, T. Lemenand, M. Khaled, Domestic thermo-electric cogeneration system optimization analysis, energy consumption and  $CO_2$  emissions reduction, *Appl. Therm. Eng.* 130 (2018) 279–295, doi:10.1016/j.applthermaleng.2017.10.148.
- [5] F. Razi, I. Dincer, Renewable energy development and hydrogen economy in MENA region: A review, *Renew. Sustain. Energy Rev.* 168 (2022) 112763, doi:10.1016/j.rser.2022.112763.
- [6] A. Giwa, M. Sheng, N. Maurice, X. Liu, Z. Wang, F. Chang, Biofuel Recovery from Plantain and Banana Plant Wastes: Integration of Biochemical and Thermochemical Approach, *J. Renew. Mater.* 11 (2023) 2593–2629, doi:10.32604/jrm.2023.026314.
- [7] A. McKay, Carbon pricing reduces inequality in pollution hazards, *Nat. Rev. Earth Environ.* 4 (2023) 434, doi:10.1038/s43017-023-00463-4.
- [8] M. Amir, S.Z. Khan, Assessment of renewable energy: Status, challenges, COVID-19 impacts, opportunities, and sustainable energy solutions in Africa, *Energy Built Environ* 3 (2022) 348–362, doi:10.1016/j.enbenv.2021.03.002.
- [9] Q. Li, C. Zheng, A. Shirazi, O. Bany Mousa, F. Moscica, J.A. Scott, R.A. Taylor, Design and analysis of a medium-temperature, concentrated solar thermal collector for air-conditioning applications, *Appl. Energy*. 190 (2017) 1159–1173, doi:10.1016/j.apenergy.2017.01.040.
- [10] M. Khaled, F. Harambat, H. Peerhossaini, Towards the control of car underhood thermal conditions, *Appl. Therm. Eng.* 31 (2011) 902–910, doi:10.1016/j.applthermaleng.2010.11.013.
- [11] M. Khaled, F. Harambat, H. Peerhossaini, Temperature and Heat Flux Behavior of Complex Flows in Car Underhood Compartment, *Heat Transf. Eng.* 31 (2010) 1057–1067, doi:10.1080/01457631003640321.
- [12] W. Salameh, C. Castelain, J. Faraj, R. Murr, H. El Hage, M. Khaled, Improving the efficiency of photovoltaic panels using air exhausted from HVAC systems: Thermal modelling and parametric analysis, *Case Stud. Therm. Eng.* 25 (2021) 100940, doi:10.1016/j.csite.2021.100940.

- [13] M.A. Green, Silicon solar cells step up, *Nat. Energy*. (2023), doi:10.1038/s41560-023-01296-7.
- [14] M. Shirinbakhsh, L.D.D. Harvey, Feasibility of achieving net-zero energy performance in high-rise buildings using solar energy, *Energy Built Environ* (2023), doi:10.1016/j.enbenv.2023.07.007.
- [15] A. Chkeir, Y. Bouzidi, Z. El Akili, M. Charafeddine, Z. Kashmar, Assessment of thermal comfort in the traditional and contemporary houses in Byblos: A comparative study, *Energy Built Environ* (2023), doi:10.1016/j.enbenv.2023.07.006.
- [16] M. Gholampour, M. Ameri, Energy and exergy analyses of Photovoltaic/Thermal flat transpired collectors: Experimental and theoretical study, *Appl. Energy*. 164 (2016) 837–856.
- [17] W. Ratismith, Y. Favre, M. Canaff, J. Briggs, A non-tracking concentrating collector for solar thermal applications, *Appl. Energy*. 200 (2017) 39–46.
- [18] J. Peng, D.C. Curcija, L. Lu, S.E. Selkowitz, H. Yang, W. Zhang, Numerical investigation of the energy saving potential of a semi-transparent photovoltaic double-skin facade in a cool-summer Mediterranean climate, *Appl. Energy*. 165 (2016) 345–356.
- [19] B. Zhao, M. Hu, X. Ao, G. Pei, Conceptual development of a building-integrated photovoltaic radiative cooling system and preliminary performance analysis in Eastern China, *Appl. Energy*. 205 (2017) 626–634.
- [20] M. Modjinou, J. Ji, J. Li, W. Yuan, F. Zhou, A numerical and experimental study of micro-channel heat pipe solar photovoltaics thermal system, *Appl. Energy*. 206 (2017) 708–722.
- [21] C. Habchi, F. Moukalled, Using AC return air for cooling PV modules in hot climate regions, in: 4th Int. Conf. Effic. Build. Des. Mater. HVAC Equip. Technol., ASHRAE, Beirut, Lebanon, 2020, p. 10.
- [22] M.U. Siddiqui, A.F.M. Arif, Electrical, thermal and structural performance of a cooled PV module: Transient analysis using a multiphysics model, *Appl. Energy*. 112 (2013) 300–312.
- [23] A. Radwan, M. Ahmed, The influence of microchannel heat sink configurations on the performance of low concentrator photovoltaic systems, *Appl. Energy*. 206 (2017) 594–611.
- [24] M.Y. Othman, A. Ibrahim, G.L. Jin, M.H. Ruslan, K. Sopian, Photovoltaic-thermal (PV/T) technology - The future energy technology, *Renew. Energy*. 49 (2013) 171–174.
- [25] K. Terashima, H. Sato, T. Ikaga, PV/T solar panel for supplying residential demands of heating/cooling and hot water with a lower environmental thermal load, *Energy Build* 297 (2023) 113408, doi:10.1016/j.enbenv.2023.113408.
- [26] A. Shahsavari, M. Arici, Energy and exergy analysis and optimization of a novel heating, cooling, and electricity generation system composed of PV/T-heat pipe system and thermal wheel, *Renew. Energy*. 203 (2023) 394–406, doi:10.1016/j.renene.2022.12.071.
- [27] W. Li, Y. Ling, X. Liu, Y. Hao, Performance analysis of a photovoltaic-thermochemical hybrid system prototype, *Appl. Energy*. 204 (2017) 939–947.
- [28] A. Shukla, K. Kant, A. Sharma, P.H. Biwole, Cooling methodologies of photovoltaic module for enhancing electrical efficiency: a review, *Sol. Energy Mater. Sol. Cells*. 160 (2017) 275–286.
- [29] S. Abdul Hamid, M. Othman, K. Sopian, S. Zaidi, An overview of photovoltaic thermal combination (PV/T) combi technology, *Renew. Sustain. Energy Rev.* 38 (2014) 212–222.
- [30] N. Aste, C. del Pero, F. Leonforte, Water flat plate (PV-)thermal collectors: A review, *Sol. Energy*. 102 (2014) 98–115.
- [31] N.A.S. Elminshawy, D.G. El-Damhogi, I.A. Ibrahim, A. Elminshawy, A. Osama, Assessment of floating photovoltaic productivity with fins-assisted passive cooling, *Appl. Energy*. 325 (2022) 119810, doi:10.1016/j.apenergy.2022.119810.
- [32] N. Elminshawy, A. Elminshawy, A. Osama, M. Bassyouni, M. Arici, Experimental performance analysis of enhanced concentrated photovoltaic utilizing various mass flow rates of Al<sub>2</sub>O<sub>3</sub>-nanofluid: Energy, exergy, and exergoeconomic study, *Sustain. Energy Technol. Assessments*. 53 (2022) 102723, doi:10.1016/j.seta.2022.102723.
- [33] K.A. Moharram, M.S. Abd-Elhady, H.A. Kandil, H. El-Sherif, Enhancing the performance of photovoltaic panels by water cooling, *Ain Shams Eng. J.* 4 (2013) 869–877.
- [34] A. Assi, A. Hassan, M. Al-Shamisi, H. Hejase, Removal of air blown dust from photovoltaic arrays using forced air flow of return air from air conditioning systems, *Renew. Energies Dev. Ctries. (REDEC)*, 2012 Int. Conf., REDEC (2012) 1–5.
- [35] M. Ebrahimi, M. Rahimi, A. Rahimi, An experimental study on using natural vaporization for cooling of a photovoltaic solar cell, *Int. Commun. Heat Mass Transf.* 65 (2015) 22–30.
- [36] M. Rahimi, P. Valeh-e-Sheyda, M.A. Parsamoghadam, M.M. Masahi, A.A. Alsairafi, Design of a self-adjusted jet impingement system for cooling of photovoltaic cells, *Energy Convers. Manag.* 83 (2014) 48–57.
- [37] H.G. Teo, P.S. Lee, M.N.A. Hawlader, An active cooling system for photovoltaic modules, *Appl. Energy*. 90 (2012) 309–315.
- [38] E. Skoplaki, J.A. Palyvos, On the temperature dependence of photovoltaic module electrical performance: A review of efficiency/power correlations, *Sol. Energy*. 83 (2009) 614–624.
- [39] BP Solar, (BP) 350 - 50 watt photovoltaic module, 2012.
- [40] S. Armstrong, W.G. Hurley, A thermal model for photovoltaic panels under varying atmospheric conditions, *Appl. Therm. Eng.* 30 (2010) 1488–1495.
- [41] ASHRAE, Standard 55-2013 - Thermal Environmental Conditions for Human Occupancy, (2013).
- [42] F.R. Menter, Two-equation eddy-viscosity turbulence models for engineering applications, *AIAA J* 32 (1994) 1598–1605, doi:10.2514/3.12149.
- [43] I.B. Celik, U. Ghia, P.J. Roache, C.J. Freitas, H. Coleman, P.E. Raad, Procedure for Estimation and Reporting of Uncertainty Due to Discretization in (CFD) Applications, *J. Fluids Eng.* 130 (2008) 78001.
- [44] ASHRAE, Fundamentals handbook, in: 2013: pp. 1–16.
- [45] Website, <https://weatherspark.com/averages/32849/Beirut-Mt-Lebanon>, (2015).
- [46] Website, <https://weatherspark.com/averages/32878/Doha-Ad-Dawhah-Qatar>, (2015).
- [47] S. Sharples, P.S. Charlesworth, Full-scale measurements of wind-induced convective heat transfer from a roof-mounted flat plate solar collector, *Sol. Energy*. 62 (1998) 69–77.
- [48] ASHRAE, Fundamentals handbook, in: 2013: pp. 1–57.
- [49] F.B. Rowley, W.A. Eckley, Surface coefficients as affected by direction of wind, *ASHVE Trans* 38 (1932) 33–45.
- [50] D.L. Evans, Simplified method for predicting photovoltaic array output, *Sol. Energy*. 27 (1981) 555–560.
- [51] J. Laufer, Investigation of turbulent flow in a two-dimensional channel, 1950.
- [52] M.A. Hasan, K. Sumathy, Photovoltaic thermal module concepts and their performance analysis: A review, *Renew. Sustain. Energy Rev.* 14 (2010) 1845–1859.
- [53] S. Farahat, F. Sarhaddi, H. Ajam, Exergetic optimization of flat plate solar collectors, *Renew. Energy*. 34 (2009) 1169–1174.
- [54] Z. Said, R. Saidur, M.A. Saba, A. Hepbasli, N.A. Rahim, Energy and exergy efficiency of a flat plate solar collector using pH treated Al<sub>2</sub>O<sub>3</sub> nanofluid, *J. Clean. Prod.* 112 (2016) 3915–3926.
- [55] A. Bejan, *Advanced Engineering Thermodynamics*, 4th ed., Wiley-Interscience, 2016.
- [56] The Appliance Nerd, How Much Water Does a Dishwasher Use?, (2021). <https://www.theappliance nerd.com/how-much-water-does-a-dishwasher-use/> (accessed April 20, 2023).
- [57] M.J. Moran, H.N. Shapiro, D.D. Boettner, M.B. Bailey, *Fundamentals of Engineering Thermodynamics*, 9th ed., Wiley, New York, 2018.